Local electronic structures of the native defects in modulation-doped AlAs/GaAs superlattices

1990 J. Phys.: Condens. Matter 2 4405

(http://iopscience.iop.org/0953-8984/2/19/008)

J. Phys.: Condens. Matter **2** (1990) 4405–4416. Printed in the UK

Local electronic structures of the native defects in modulation-doped AlAs/GaAs superlattices

En-Ge Wang†‡, Wei-Min Jin§, Li-Yuan Zhang‡ and Huai-Yu Wang‡

† Centre of Theoretical Physics, CCAST (World Laboratory), Beijing, People's Republic of China

‡ Department of Physics, Peking University, Beijing 100871, People's Republic of China‖

§ Institute of Physics, Academia Sinica, PO Box 603, Beijing 100080, People's Republic of China

Received 20 October 1989, in final form 8 January 1990

Abstract. We investigate the character of the native defects (antisites, interstitials, vacancies and complexes of these or with impurities) in undoped and n- or p-type modulation-doped AlAs/GaAs superlattices by means of the developed recursion method. The presented electronic structures, and local and partial density of states give us a detailed identification of these defects in various types of AlAs/GaAs superlattice. We have calculated the energies of highly localised electronic states and compared the results with the existing theoretical and experimental data. The stable states of the EL2 defect (As_{Ga}–I_{As} pair) are studied under the assumption that it has the same atomic configuration as that in the bulk GaAs. With respect to the energy distribution, the electronic occupancy of various defects and of their atomic orbitals are determined; these show the occupied charge states directly. On the basis of these calculations, we find that the ionicity of a normal group III or V atom in AlAs/GaAs superlattices will be always positive when it becomes an interstitial and will be changed with different type of doping when it becomes an antisite. By considering the coulombic nature of a Frenkel pair, some specific complexes between the native defects themselves or with the impurity Si are suggested. Finally, we describe the self-diffusion and the impurity diffusion mechanisms which occur in AlAs/GaAs superlattices with and without doping. Our results are compared and contrasted with those of the bulk GaAs materials.

1. Introduction

The study of native defects (impurities, vacancies, interstitials, antisites and complexes of these) in semiconductor materials has played a key role in the construction of various electronic devices and integrated circuits. This is because small amounts of defects can drastically change the optical and transport properties of semiconductors, especially in multilayer systems.

The effort to understand different point defect mechanisms in the bulk material has long been known [1, 2]. A study of this field shows that there are shallow and deep localised states in the energy gap of semiconductors with various defects. With the development of thin-film growth techniques such as MBE or MOCVD, growing attention has been paid to experimental and theoretical investigations of the same problem in semiconductor superlattices. Many interesting results for different impurities in AlAs/GaAs multilayer systems have been contributed by some researchers [3–7]. Of these,

‖ Address to which all correspondence should be sent.

0953-8984/90/194405 + 12 $03.50

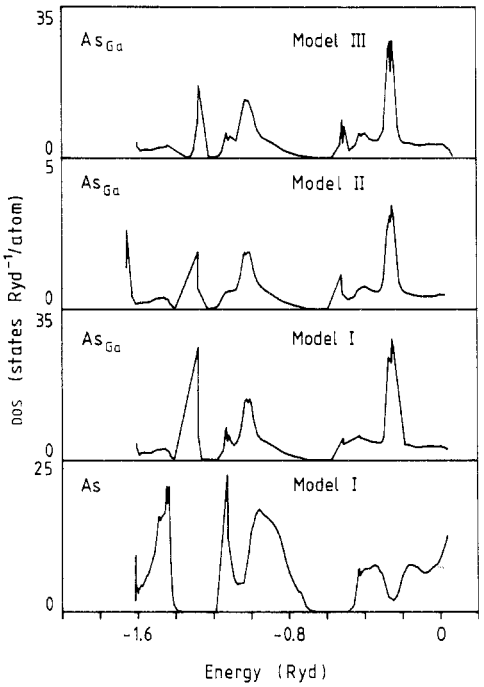

Figure 1. LDOS of an As_{Ga} antisite defect in models I, II and III, where the LDOS of an As atom in model I serves as a 'reference'.

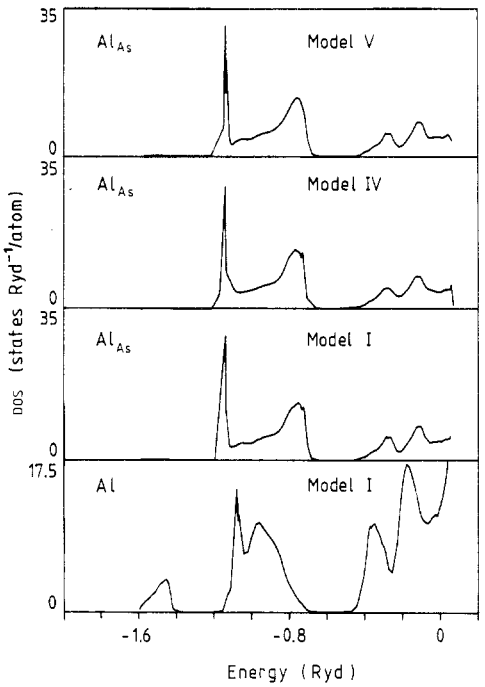

Figure 2. LDOS of an Al_{As} antisite defect in models I, IV and V, where the LDOS of an Al atom in model I serves as a 'reference'.

Nelson *et al* [6] and we [7] studied the impurity states in heavily and lightly doped AlAs/GaAs superlattices using different methods, respectively. Recently, we [8, 9] have reported the influence of vacancies on the electronic properties of AlAs/GaAs systems. However, to our knowledge, the antisites, the interstitials and some complexed defects in these structures have scarcely been studied up to now. Do they not exist in doped and undoped AlAs/GaAs superlattices? The answer is certainly yes. In our recent experiments [8] on low-temperature quantum transport of the two-dimensional electron gas in fast and thermal neutron-irradiated $Al_xGa_{1-x}As/GaAs$ modulation-doped heterojunctions, we found that there are a large number of defects, such as the antisite As_{Ga} configuration and complexes of elementary point defects. Under strong magnetic fields, they broaden the Hall plateaux associated with the localised states [8]. Therefore, it is interesting to report a more detailed study of the influence of such defects on the physical properties of AlAs/GaAs multilayer systems.

Some first-principles calculations have been performed for these defects [1, 2]. However, most of these have only addressed problems in the bulk materials. For this reason, one aim of the paper is to give a detailed description of the electronic structure, which is the characteristic function of most properties of semiconductors including the binding energy, photoemission spectra, and magnetism of the native defects in both doped and undoped AlAs/GaAs superlattices. In addition, the identification of different native defects in semiconductor superlattices is a primary goal. We believe that the results presented which are based on the local density of states (LDOS), the partial density of states (PDOS) and the electronic occupancy (EO) that have not been examined before on various defects will show their characteristics clearly.

The main features of this paper can be outlined as follows. A brief review of the calculation method is given in section 2, where we have also checked the validity of our

Table 1. Characteristics of native defects in five models of undoped and n- or p-type Si modulation-doped AlAs/GaAs superlattices. The Fermi energies for different models are also given. The zero of the energy scale is defined at infinite distance.

Model	Geometry	Fermi level (Ryd)	Defects	
			Cations	Anions
I	$(AlAs)_3/(GaAs)_3$	−0.6534	As_{Ga}, As_{Al}, $I_{As}(1)$, $I_{As}(2)$, $I_{As}(3)$, $I_{Ga}(1)$, $I_{Ga}(2)$, $I_{Al}(1)$, $I_{Al}(3)$, V_{As}	Ga_{As}, Al_{As}, V_{Al}, V_{Ga}
II	n-type Si–$(AlAs)_3/(GaAs)_3$	−0.5180	As_{Ga}, As_{Al}, Si_{Al}, As_{Si}, Al_{Si}	Ga_{As}, Al_{As}, Si_{As}, V_{Al}, V_{Ga}, V_{As}
III	p-type Si–$(AlAs)_3/(GaAs)_3$	−0.6610	As_{Ga}, As_{Al}, Si_{Al}, V_{Al}, V_{Ga}, V_{As}	Ga_{As}, Al_{As}, Al_{Si}, Si_{As}, As_{Si}
IV	n-type Si–$(GaAs)_3/(AlAs)_3$	−0.5489	As_{Ga}, As_{Al}, Si_{Ga}, Ga_{Si}, As_{Si}	Ga_{As}, Al_{As}, Si_{As}, V_{Al}, V_{Ga}, V_{As}
V	p-type Si–$(GaAs)_3/(AlAs)_3$	−0.6637	As_{Ga}, As_{Al}, Si_{Ga}, V_{Al}, V_{Ga}, V_{As}	Ga_{As}, Al_{As}, Ga_{Si}, Si_{As}, As_{Si}

mechanism by comparison with the results of Min *et al* [10] from the self-consistent full-potential linearised augmented-plane-wave (FLAPW) band calculation. The detailed description of the recursion method can be seen in Haydock's work [11] and our earlier papers [9, 12]. It has led to the development of a powerful and accurate calculation for the electronic structure of materials containing defects many of which are outside the reach of methods based on Bloch's theorem. Five models of undoped and n- and p-type modulation-doped AlAs/GaAs superlattices have been invoked in the discussion of various native defects contained in these materials, as we shall see in section 3. The main attention has concentrated on interstitial, antisite and complex defects for simple impurities and vacancies were investigated in our previous work (see [7] and [9], respectively). We have calculated the LDOSs and PDOSs of the defects possible in the five models. They are antisites (As_{Ga}, As_{Al}, As_{Si}, Ga_{As}, Ga_{Al}, Ga_{Si}, Al_{As}, Al_{Ga}, Al_{Si}, Si_{As}, Si_{Ga} and Si_{Al}, interstitials ($I_{As}(j)$, $I_{Ga}(j)$ and $I_{Al}(j)$, where $j = 1, 2, 3$ stands for when four nearest neighbours are As, Ga or Al atoms, respectively) and vacancies (V_{As}, V_{Al} and V_{Ga}). In addition, some typical complexes such as As_{Ga}–I_{As} and Si_{III}–V_{III} in diffusion processes are also studied. The calculated EOs of different lattice sites show the charge states of these defects directly. On the basis of the calculation of the charge states, we have suggested some other complexes due to the Coulomb interaction. Furthermore, the possible mechanisms of self-diffusion and impurity diffusion in AlAs/GaAs superlattices with and without doping are discussed. Section 4 gives the conclusion of the present paper.

2. Model and method

In this paper, the local electronic structure of native defects (antisites, interstitials, vacancies and complexes of these or with impurities), in the middle of the wells or barriers, in five models of undoped and n- or p-type modulation-doped AlAs/GaAs superlattices are calculated. The detailed characteristics are given in table 1; special attention should be paid to the model numbers for reference during the following discussion. We now explain their meaning, using model IV as an example. The n-type Si–

$(GaAs)_3/(AlAs)_3$ model is used for the heavily doped $(GaAs)_3/(AlAs)_3$ ordered structure, where there is one Ga atom layer substituted by a Si atom layer in every superlattice period along the (001) growing direction. The cases are the same as those given in figure 1 of [6]. In each model, we determine the Fermi level by the integration of the total density of states (TDOS). The zero of the energy scale is defined at infinite distance.

The recursion method [11] used here is a well known approach to calculate the electronic structure of materials. Specifically, it is suitable to find local details of point defects contained in these crystals [7, 9] (for a review see [13]). Because, in these cases, the small quantity of defects break down the periodic symmetry, the general band-structure calculations based on Bloch's theorem do not easily provide a well defined and converged treatment. In spite of the accuracy of the results obtained through the applications of some band-structure calculation methods to specific cases, the artificial use of periodically repeating supercells can become essentially impractical. In this paper, we first introduce the recursion method to present the local nature of native defects contained in doped and undoped AlAs/GaAs superlattices.

In order to check the validity of our calculation procedure, we calculated the $(AlAs)_1/(GaAs)_1$ superlattice within the tight-binding formalism using the parameter set of Harrison [14] and compared the results with those of Min *et al* [10] from the self-consistent FLAPW band calculation. We found that the agreement between these results is good. In the energy band calculation, only one cell is considered for the approximation of the periodic boundary condition. This is not equivalent to treating sufficiently large-size clusters. In our performance, the atom cluster containing about 5000 sites is taken as an imitation of a real crystal which has no boundary, and the recurrence chain length is selected as $L = 30$ [9, 12] by checking the convergence through calculations truncated at different maximum L.

There are various methods of determining the atomic valence of an atom in the crystals, but two of these methods are usually used by theorists [15]. One is to determine the space distribution of the valence electron density. Based on the assumed atomic radius, the valence can be found by the integration within atomic sphere, but this method cannot easily be used to divide exhaustively all valence electrons in the crystal in a rational way (see e.g. [16]). The other method [17] is to determine the energy distribution of valence electronic density of states (DOS). Because the integration of the TDOS up to E_F should equal the number of total valence electrons, this method leaves no extra electrons in the crystal.

In this paper, we consider the valence electron number n_l that one atom possesses by integrating its electronic DOS up to Fermi level. Then apparently with respect to the energy distribution, the atomic valence of l atoms is given by

$$\Delta N_l = N_l - n_l = N_l - \frac{1}{N} \sum_{\alpha, E_n \leq E_F} |\varphi^{\alpha}_{n(l)}|^2$$

where N_l is the number of valence electrons on the free atom l, and $\varphi^{\alpha}_{n(l)}$ is the component of the eigenfunction corresponding to the valence orbital α on this atom. Using this method we [12] have calculated the atomic valence in the high-T_c material Y–Ba–Cu–O. Our results are in fair agreement with the values adopted by Chaplot [18] in his calculation of the phonon dispersion relation of the same superconductor, which was confirmed by various experiments.

3. Results and discussion

3.1. Group III and V antisite defects

Using the method discussed in section 2, we calculated the LDOS of antisites in both group III and group V substructures in undoped and n- or p-type modulation-doped

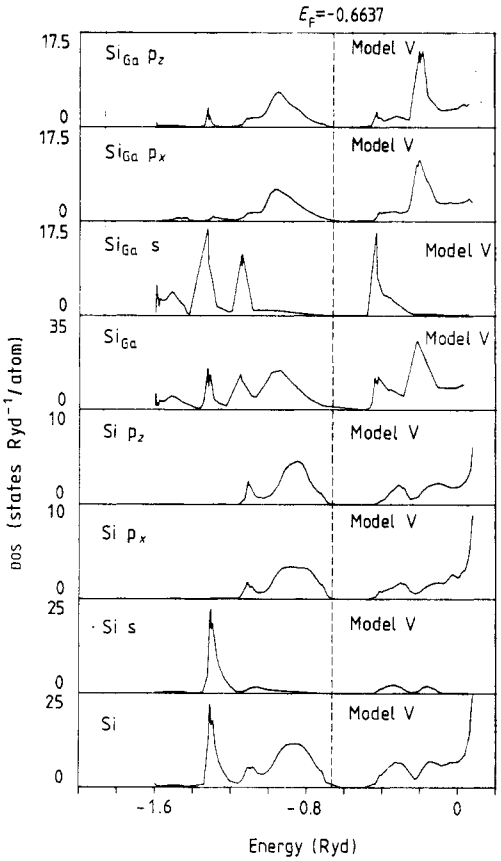

Figure 3. LDOSs and PDOSs of a Si_{Ga} antisite defect in model V, where the LDOS and PDOS of a Si atom in model V serve as 'references'. Si_{Ga} p_x stands for the p_x partial wave of the Si_{Ga} antisite.

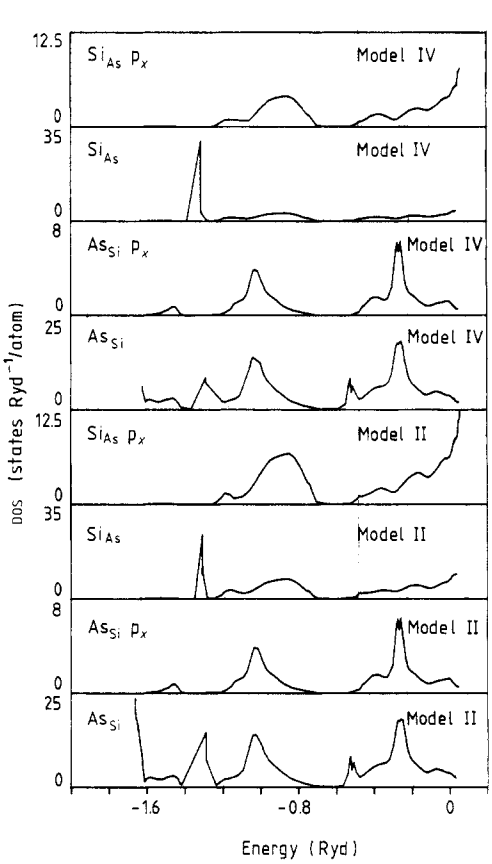

Figure 4. LDOS and p_x DOSs of Si_{As} and As_{Si} in models II and IV.

AlAs/GaAs superlattices. Some results of antisite defects and an As or Al 'reference atom' are shown in figures 1 and 2. It is easy to see that the splitting of s and p valence bands of antisites disappears for s states shifting towards the Fermi level. The LDOS shapes of the conduction band of As_{Ga} defects are very similar to that of Si donors [7]. We believe that As_{Ga} is a donor-like defect. The deep levels of antisite As_{Ga} in undoped, n-type doped and p-type doped materials were discovered at $E_c - 0.80$ eV, $E_c - 1.10$ eV and $E_c - 0.95$ eV, respectively. While the Si level is at $E_c - 0.1$ eV in n-type AlAs/GaAs superlattice [6].

Figure 2 shows the local DOS of the acceptor-like Al_{As} antisite defects in models I, IV and V. We find the acceptor levels at $E_v + 0.54$ eV and $E_v + 0.33$ eV for models IV and V, respectively. We have also calculated the localised levels of Ga_{As} defects, e.g. $E_v + 0.30$ eV in p-type materials. In this case, our calculation is more similar to the observations of Yu [19] and Elliott [20] ($E_v + 0.23$ eV) in the bulk than to those of Wang [21] ($E_v + 0.70$ eV). The main contribution to the shifting of the valence band top originates from p states of Al_{As} and Ga_{As} defects.

In order to discuss the behaviour of group III and V antisite defects in more detail, we determined the valence electron number on each antisite in five models by integrating

Table 2. EOs of a group III or V antisite in undoped and n- or p-type Si modulation-doped AlAs/GaAs superlattices.

	EO for the following models				
Antisite	I	II	III	IV	V
As_{Ga}	4.19	4.33	4.66	4.25	4.41
As_{Al}	4.20	4.35	4.78	4.25	4.20
Ga_{As}	3.82	3.82	3.85	3.58	3.85
Al_{As}	3.86	3.86	3.90	3.86	3.86

Table 3. EOs in partial waves of native defects in undoped and n- or p-type Si modulation-doped AlAs/GaAs superlattices.

		EO in the following partial waves			
Model	Point defects	s	p_x	p_y	p_z
I	$I_{As}(1)$	1.87	0.552	0.552	0.593
	$I_{As}(2)$	1.83	0.905	0.905	0.940
	$I_{As}(3)$	1.83	0.951	0.950	0.855
	$I_{Ga}(1)$	1.66	0.345	0.345	0.345
	$I_{Ga}(2)$	1.63	0.305	0.305	0.392
	$I_{Al}(1)$	1.18	0.346	0.347	0.346
	$I_{Al}(3)$	1.57	0.307	0.307	0.307
II	As_{Ga}	1.74	0.862	0.862	0.862
	Si_{As}	1.49	0.924	0.924	0.926
III	Ga_{As}	1.38	0.824	0.824	0.825
	Al_{Si}	1.31	0.865	0.865	0.862
IV	Al_{As}	1.30	0.853	0.853	0.852
	As_{Si}	1.48	0.904	0.903	0.897
V	As_{Al}	1.61	0.865	0.865	0.865
	Si_{Ga}	1.41	0.798	0.798	0.792

their electronic DOSs up to the Fermi level (table 2). Some corresponding results for every atomic orbital on these antisites are given in table 3. First of all, we show that the ionicity of a group III or V atom in AlAs/GaAs superlattices will be changed when it becomes an antisite defect. We now explain this using As_{Ga} and As_{Al} as examples. In model V of the p-type modulation-doped AlAs/GaAs superlattice, the EO of As_{Ga} and As_{Al} defect are about 4.41 and 4.20 (fewer than 5 electrons), but that of an As atom is about 5.13 (more than 5 electrons). Therefore the As_{Ga} and As_{Al} antisite defects are expected to act as donors, while Ga_{As} and Al_{As} act as acceptors, which is consistent with the arguments discussed above.

3.2. Impurity antisite defects

Silicon on the group III atom substructure in $Al_xGa_{1-x}As$/GaAs quantum well heterostructures has been suggested by several studies [22]. We have discussed all the possible impurity antisite defects both for Si impurities on the group III or V atom sublattice and for group III or V atoms on the Si sublattice in four periodic modulation-doped AlAs/GaAs superlattices (i.e. models II–V). As shown earlier, we consider

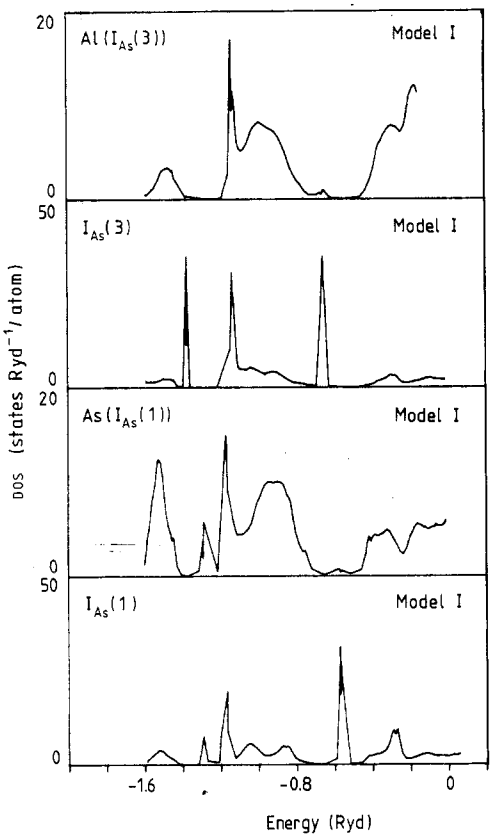

Figure 5. LDOSS of $I_{As}(1)$, $I_{As}(3)$ and their neighbours in model I, where $As(I_{As}(1))$ or $Al(I_{As}(3))$ represents the neighbour of the interstitial $I_{As}(1)$ or $I_{As}(3)$ respectively.

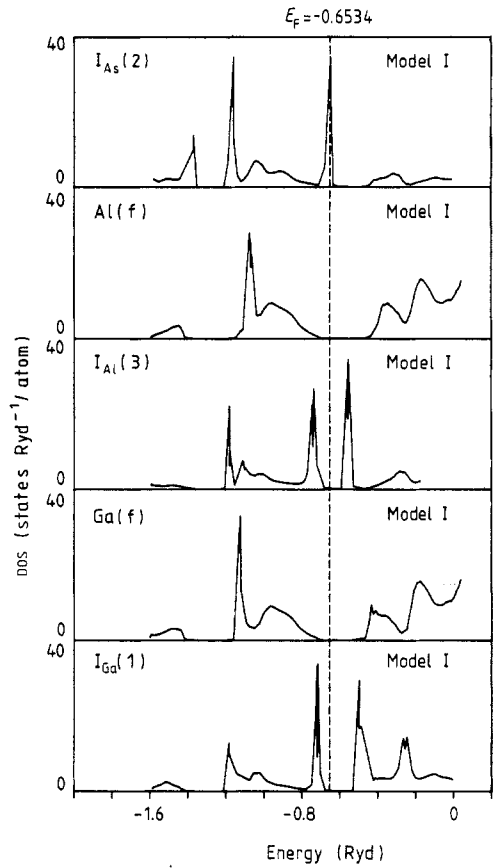

Figure 6. LDOSS of the interstitials in model I. The LDOSS of Al(f) and Ga(f) atoms in the same model serve as 'references', where the label f represents the atom far from the interstitials.

in detail only some calculated results, although other cases may also have the same importance.

Figure 3 shows the local and partial DOSS of antisite Si_{Ga} in model V, where the Fermi level is at -0.6637 Ryd. The shifting value of the peak at the conduction band near the gap is about 1.63 eV in this model. We find that the Si_{III} defect influences mainly the conduction band, but the Si_V defect influences the valence band in both n- and p-type modulation-doped superlattices.

We now also discuss the local electronic structure when an As atom is on the Si sublattice in both the GaAs and the AlAs regions of n-type materials (figure 4). This clearly shows that the results are almost the same in two cases, which reflects a similar bonding picture around Ga or Al atoms. By comparison with As_{Ga} of model II in figure 1, we find that the antisite As_{Si} is donor like. The corresponding defect level is localised at $E_c - 1.01$ eV, which is shallower than that of the As_{Ga} defect, but this is not always true for p-type material, as will be clear from the following discussion.

The EOS of various impurity antisite defects are given in table 4. It is easy to see that Si_{III} is donor like and Si_V is acceptor like in both n- and p-type AlAs/GaAs superlattices. However, a group III atom on the Si sublattice will act as a donor in n-type doped

Table 4. EOs on an antisite, which is related to a Si impurity, in various types of modulation-doped AlAs/GaAs superlattice.

Model	Defect	EO	Defect	EO	Defect	EO	Defect	EO
II	Si_{Al}	3.57	Al_{Si}	2.84	Si_{As}	4.26	As_{Si}	4.36
III	Si_{Al}	3.91	Al_{Si}	3.90	Si_{As}	4.59	As_{Si}	5.15
IV	Si_{Ga}	3.55	Ga_{Si}	2.97	Si_{As}	4.18	As_{Si}	4.18
V	Si_{Ga}	3.79	Ga_{Si}	3.85	Si_{As}	4.46	As_{Si}	5.04

materials and as an acceptor in p-type doped materials. This will also be seen when As_{Si} defects are in different doping structures. The reason that the ionicity of the same antisite defect will change with different doping types is that its valence electrons depend sensitively on the position of the Fermi level. This is important because it can illustrate the nature of complexes involving the interaction of primary defects with impurities.

3.3. Interstitials

The description of the electronic structure of interstitials is important because their local atomic configuration will be changed significantly. Here we have studied the interstitials $I_{As}(j)$, $I_{Ga}(j)$ and $I_{Al}(j)$ in the AlAs/GaAs superlattice, where $j = 1, 2, 3$ stands for when the four nearest neighbours are As, Ga or Al atoms, respectively.

To investigate the local electronic structure of these defects and to see the influence on their neighbours, we show the LDOS in figure 5. As ($I_{As}(1)$) represents an As atom near to the interstitial $I_{As}(1)$, by comparison with an As atom in model I we can see that there are several associated localised levels in the forbidden gap. We find that the $I_{As}(1)$ interstitial levels are in the middle of the energy gap and the peaks of the $I_{As}(2)$ and $I_{As}(3)$ LDOS across the Fermi level (-0.6534 Ryd). It should be pointed out that we do not consider the lattice distortion in this case. Of course a definitive test of the validity of our proposal must be experimental. As this has not yet been achieved, we have performed fairly detailed calculations.

The LDOSS and PDOSS of group III interstitials are shown in figures 6 and 7, respectively. The defect levels are discovered at $E_c - 0.54$ eV for $I_{Ga}(1)$ and $E_c - 1.90$ eV for $I_{Al}(3)$. In figure 7 we find that the contribution to the LDOS peak of the conduction band originates from p states and the peak of the valence band from s states. The cases are very similar to that of the vacancy-induced structure of AlAs/GaAs superlattices [9]. We can understand the character with simple bonding pictures. Because of the existence of broken hybrid sp bonds on interstitial atoms, the distribution of the local charge density will be changed. We believe that it is possible for extra p electrons to occupy the non-bonding states.

On the basis of our calculation of the EO of an interstitial defect, we find that all the possible group III or V interstitials in the AlAs/GaAs superlattice are in positive charge states. Therefore, they are donors, which is in agreement with the results of Baraff and Schluter [23] and in contrast to some analyses which assumed that I_{Ga} is an acceptor.

3.4. Complexes and diffusion mechanisms

Recent experiments have shown that some electrical and optical characteristics of $Al_xGa_{1-x}As/GaAs$ quantum well heterostructures and superlattices result from complexes formed by the interaction of simple point defects between themselves or with impurities. Here we use the model for the stable state in GaAs material, which has been

reduced. The total spin singlet ground state is substantially lower in energy than the 'Zhang and Rice' solution and in view of the considerations above this is the expected ground state for the lattice. Moreover the cluster calculation that the spin singlet state is stable with respect to the 'Zhang and Rice' state for $\Delta > 0.37U$ is probably a lower bound on Δ. Finally, the Bloch momentum of the hole is expected to be at the non-interacting Fermi surface in the low-spin case.

What has this calculation to say about the real cuprate superconductors? Experimentally it is observed that the undoped materials have a long-range staggered magnetisation which is very well explained by a spin-$\frac{1}{2}$ Heisenberg Hamiltonian with an antiferromagnetic exchange coupling constant $J \simeq 300$ K (Chakravarty *et al* 1989). Thus a model describing holes doped into the copper oxide planes should have an antiferromagnetic Heisenberg term. As holes are doped into the planes, the antiferromagnetic correlations are scrambled so that for sufficient concentration (~ 0.1) the Néel ordering is destroyed, although it is not yet known which spin correlations replace the Néel ones.

In the t–J model one may qualitatively picture this as arising from polaronic distortions of the Néel ordering due to the propagating holes. There is a competition between minimising the kinetic energy of the holes (which means delocalising the hole in a region determined by Nagaoka phase coherence) and maximising the energy gained from Néel ordering. Since the kinetic energy of the holes prefer high spin, and antiferromagnetic interactions prefer low spin, these processes are at variance with one another.

In contrast to this the kinetic energy of the hole in the two-band model with virtual Cu^{1+} excitations and the t–t'–J model (namely both frustrated) prefer low spin and therefore there is less competition with the super-exchange. Thus, while all three models may well predict low-spin polaronic distortions of the Néel order (provided J/t is not vanishingly small in the t–J model) the internal structure of these polarons may be quite different in the frustrated models and unfrustrated model.

Acknowledgment

The author wishes to especially thank Dr M W Long for many useful discussions, hints and suggestions.

Appendix. The non-orthogonality of the basis states

In this appendix the overlap of the basis states (3.1) are shown. The relevant part of the basis states are represented in the following by $|ij\rangle$ where i and j represent nearest-neighbour lattice positions. Thus, $\langle S+|+S\rangle = \frac{1}{8}$ shows that a state with a singlet quasiparticle on the ith site and an up spin on the jth site has an overlap of one eighth with

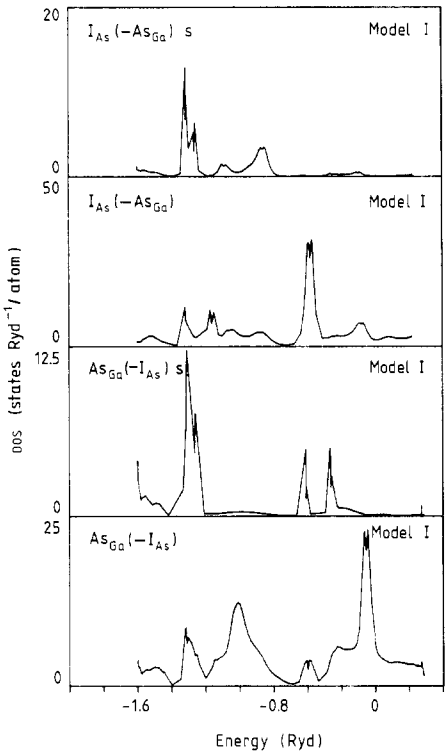

Figure 8. LDOSS and s PDOSS of As_{Ga} and I_{As} in the As_{Ga}–I_{As} stable state, where $I_{As}(-As_{Ga})$ or $As_{Ga}(-I_{As})$ represents the I_{As} interstitial or As_{Ga} antisite in this As_{Ga}–I_{As} pair respectively.

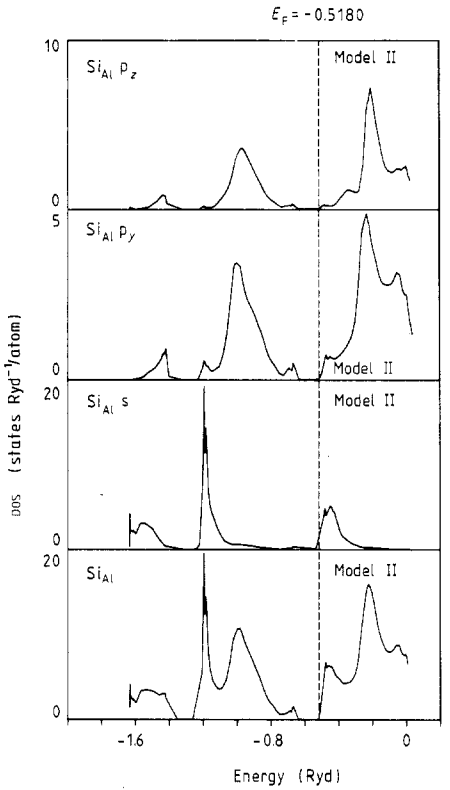

Figure 9. LDOSS and PDOSS of Si_{Al} antisite in the (Si_{Al}–V_{Al}) complex of model II.

Table 5. EOS on an interstitial and its neighbour atom in AlAs/GaAs superlattices.

Interstitial	EO	Neighbour of interstitial	EO
$I_{As}(1)$	3.57	$As(I_{As}(1))$	4.91
$I_{Ga}(1)$	2.70	$As(I_{Ga}(1))$	4.99
$I_{Al}(1)$	2.22	$As(I_{Al}(1))$	5.08
$I_{As}(2)$	4.58	$Ga(I_{As}(2))$	3.08
$I_{Ga}(2)$	2.63	$Ga(I_{Ga}(2))$	3.10
$I_{As}(3)$	4.59	$Al(I_{As}(3))$	2.97
$I_{Al}(3)$	2.49	$Al(I_{Al}(3))$	3.00

The lattice atom self-diffusion and the impurity diffusion must proceed through native defects in the crystal. Studies of the important defect mechanisms that control diffusion in AlAs/GaAs superlattices have been presented in a number of characterisation techniques [25–27]. From our previous work [9], we know that the V_{III} vacancy is a negatively charged acceptor and the V_V vacancy is a positively charged donor in the AlAs/GaAs superlattice. On the basis of the results given in table 5, we believe that the V_{III}^{-}–I_{III}^{+} Frenkel pair will be formed in the AlAs/GaAs superlattice. The self-diffusion

of group III defects (V_{Ga}, V_{Al}, I_{Ga} and I_{Al}) in these multilayer systems occurs through the simple reactions, which are similar to that of bulk GaAs material [28]:

$$V_{III} \rightleftharpoons V_{III} + (I_{III'} + V_{III'}) \rightleftharpoons (V_{III} + I_{III'}) + V_{III'} \rightleftharpoons V_{III'}$$

or

$$I_{III} \rightleftharpoons I_{III} + (V_{III'} + I_{III'}) \rightleftharpoons (I_{III} + V_{III'}) + I_{III'} \rightleftharpoons I_{III'}.$$

However, this procedure is hardly performed by group V defects. This is because I_{As} is also a positively charged donor, just like the V_{As} vacancy. So the Frenkel pair V_V^+–I_V^+ cannot be formed by coulombic attraction in the undoped AlAs/GaAs superlattice, but the charged states of group III and group V vacancies may be changed with different types of doping (see table 1 and [29]).

The Si diffusion, and the layer intermixing in $Al_xGa_{1-x}As$/GaAs superlattices that accompanies the Si diffusion, are suggested by Deppe *et al* [22] to occur via group III vacancies, which are generated by Frenkel defects. In our present results in table 4, it is clearly shown that Si_{III} is a positively charged donor in both n- and p-type modulation-doped AlAs/GaAs superlattices. Therefore, because of the coulombic attraction, there is a significant probability that Si_{III} forms a complex with a V_{III} vacancy: $Si_{III}^+ + V_{III}^- \rightleftharpoons Si_{III}^+$–$V_{III}^-$. This agrees with the assumption of Deppe *et al* [28]. Among the possible vacancies and interstitials in the AlAs/GaAs superlattices, only V_{III} is expected to have acceptor-like energy states. The group III vacancy plays a major role in diffusion mechanisms. We consider the Si_{Al}^+–V_{Al}^- complex in more detail and give the LDOS and PDOS of the Si_{Al} defect of this pair for model II in figure 9. The shifts of the bottom of conduction band and the top of valence band towards the Fermi level are about 0.68 eV and 0.19 eV, respectively. Furthermore, we have shown that Si_V is a negatively charged acceptor. Therefore we believe that there is another kind of complex formed in AlAs/GaAs superlattices, which can be written as: $Si_V^- + V_V^+ \rightleftharpoons Si_V^- - V_V^+$. Both Si_{III}^+–V_{III}^- and Si_V^-–V_V^+ are thought to be the mobile species by which the Si diffuses, where the Si_{III} or Si_V isolated acceptor or donor will be immobile.

On the assumption of the complexes formed owing to the coulombic interaction and the calculated atomic valence of the native defects considered here, we can suggest some other complexes, such as As_{III}^+–V_{III}^-, Ga_{As}^-–V_{As}^+ and Al_{As}^-–V_{As}^+, in undoped and p- or n-type modulation-doped AlAs/GaAs superlattices. Also, there will be some III_{Si}^+–V_{III}^- and As_{Si}^+–V_V^- complexes in n-type doped materials and some III_{Si}^-–V_{III}^+ and As_{Si}^-–V_V^+ complexes in p-type doped materials. These have been observed in recent experiments [30, 31].

4. Conclusions

We have presented a calculation of the LDOSs and PDOSs of the native defects (such as antisites, interstitials, vacancies and complexes of these or with impurities) in undoped and p- or n-type modulation-doped AlAs/GaAs superlattices and used these results to examine the influence of these defects on the charge distributions of their neighbour atoms, and to obtain a prediction for the behaviour of such defects (see table 1). The shift of the LDOS towards the Fermi level suggests that there are some localised states in the forbidden gap, and their positions are discovered for different antisites, interstitials, vacancies and complexes. Our results confirm most of the earlier theoretical calculations and experimental data, while we give more details of the nature of these defects in doped and undoped AlAs/GaAs superlattices.

With respect to the energy distribution, we calculate the valence electron number on each defect atom and its partial orbitals by integrating the electronic LDOS and PDOS

up to Fermi level. These results clearly show the properties of the charge states which the native defects occupy. From the discussion of the atomic valence, we find that As_{III} and Si_{III} are donor like in all cases, while Ga_V, Al_V and Si_V are acceptor like. However, the charged states of Ga_{Si}, Al_{Si} and As_{Si} antisites depend on doping type, just like vacancies. By coulombic attraction, we explain the nature of the Frenkel pair V_{III}^{-}–I_{III}^{+}, which is an important mechanism for controlling self-diffusion in AlAs/GaAs superlattices, and why V_V^{+}–I_V^{+} pairs are hardly formed in such materials. Besides the Si diffusion via group III vacancies suggested by Deppe *et al*, we find that it is possible that Si diffusion proceeds with group V vacancies, i.e. Si_V^{-}–V_V^{+}. Furthermore, from our calculations, we confirm that other complexes do exist in doped and undoped AlAs/GaAs superlattices, and these have been observed in recent experiments.

References

[1] Lannoo M and Bourgion J C 1981 *Points Defects in Semiconductors* vol I *Theoretical Aspects* (Berlin: Springer)
[2] Bourgion J C and von Bardeleben H J 1988 *J. Appl. Phys.* **64** R65
[3] Bastard G 1981 *Phys. Rev.* B **24** 4714
[4] Masselink W T, Chang Y C and Morkoc H 1985 *Phys. Rev.* B **32** 5190
[5] Deppe D G, Nam D W, Holonyak N Jr, Hsieh, K C, Baker J E, Kuo C P, Fletcher R M, Osentowski T D and Craford M G 1988 *Appl. Phys. Lett.* **52** 1413
[6] Nelson J S, Fong C Y, Batra I P, Pickett W E and Klein B M 1988 *Phys. Rev.* B **37** 10203
[7] Wang En-Ge, Zhang Li-Yuan and Wang Huai-Yu 1989 *J. Phys.: Condens. Matter* **1** 8065; 1990 *Mater. Sci. Eng.* B at press
[8] Jin Wei-Min, Zhou Jun-Ming, Huang Yi and Cai Li-Hong 1988 *Phys. Rev.* B **38** 13086, 13090
[9] Wang En-Ge, Zhang Li-Yuan and Wang Huai-Yu 1989 *Phys. Status Solidi* **155** 363
[10] Min B I, Massidda S and Freeman A J 1988 *Phys. Rev.* B **38** 1970
[11] Haydock R 1980 *Solid State Physics* vol 35 (New York: Academic) p 216
[12] Wang Huai-Yu, Liu Fu-Sui and Wang Cong-Yu 1989 *J. Phys.: Condens. Matter* **1** 1983
[13] 1984 *Solid State Sci.* **58**
[14] Harrison W H 1980 *Electronic Structures and the Properties of Solids* (San Francisco: Freeman)
[15] Wang Huai-Yu, Lui Fu-Sui, Wang En-Ge and Wang Chong-Yu 1990 *Z. Phys.* B at press
[16] Herman F, Kasowski R V and Hsu W Y 1987 *Phys. Rev.* B **36** 6904
[17] Richert B A and Allen R E 1988 *Phys. Rev.* B **37** 7496
[18] Chaplot S L 1988 *Phys. Rev.* B **37** 7435
[19] Yu P W, Mitchel W C, Mier M G, Li S S and Wang W L 1982 *Appl. Phys. Lett.* **41** 532
[20] Elliott K R, Holmes D E, Chen R T and Kirkpatrick C G 1982 *Appl. Phys. Lett.* **40** 898
[21] Wang Z G, Lebedo L A and Grimmeiss H G 1984 *J. Phys. C: Solid State Phys.* **17** 259
[22] Deppe D G, Holonyak N Jr, Kish F A and Baker J E 1987 *Appl. Phys. Lett.* **50** 998 and references therein
[23] Baraff G A and Schluter M 1985 *Phys. Rev. Lett.* **55** 1327
[24] Meyer B K, Hofmann D M, Niklas J R and Spaeth J M 1987 *Phys. Rev.* B **36** 1332
[25] Baraff G A and Schluter M 1987 *Phys. Rev.* B **35** 6154
[26] Camras M D, Holonyak N Jr, Burnham R D, Streifer W, Scifres D R, Paoli T L and Lindstrom C 1983 *J. Appl. Phys.* **54** 5637
[27] Schlesinger T E and Kuech T 1986 *Appl. Phys. Lett.* **49** 519
[28] Deppe D G, Holonyak N Jr, Plano W E, Robbins V M, Dallesasse J M, Hsieh K C and Baker J E 1988 *J. Appl. Phys.* **64** 1838
[29] Tan T Y and Gosele U 1987 *J. Appl. Phys.* **61** 1841
[30] Mei P, Yoon H W, Venkatesan T, Schwarz S A and Harbison J P 1987 *Appl. Phys. Lett.* **50** 1823
[31] Tan T Y and Gosele U 1988 *Appl. Phys. Lett.* **52** 1240